minerals

MDPI

Article

Ciriottiite, $Cu(Cu,Ag)_3Pb_{19}(Sb,As)_{22}(As_2)S_{56}$, the Cu-Analogue of Sterryite from the Tavagnasco Mining District, Piedmont, Italy

Luca Bindi [1,*], Cristian Biagioni [2], Bruno Martini [3] and Adrio Salvetti [3]

[1] Dipartimento di Scienze della Terra, Università degli Studi di Firenze, Via G. La Pira 4, I-50121 Firenze, Italy
[2] Dipartimento di Scienze della Terra, Università di Pisa, Via Santa Maria 53, I-56126 Pisa, Italy; biagioni@dst.unipi.it
[3] Associazione Micromineralogica Italiana, Via Gioconda 3, I-26100 Cremona, Italy; bruno.martini49@tiscali.it (B.M.); angela.adrio@libero.it (A.S.)
* Correspondence: luca.bindi@unifi.it; Tel.: +39-055-275-7532

Academic Editor: Federica Zaccarini
Received: 29 December 2015; Accepted: 28 January 2016; Published: 1 February 2016

Abstract: The new mineral species ciriottiite, ideally $Cu(Cu,Ag)_3Pb_{19}(Sb,As)_{22}(As_2)S_{56}$ has been discovered in the Tavagnasco mining district, Piedmont, Italy, as very rare black metallic tubular crystals, up to 150 μm in length, associated with Bi sulfosalts and arsenopyrite. Its Vickers hardness (VHN_{10}) is 203 kg/mm^2 (range 190–219). In reflected light, ciriottiite is light grey in color, distinctly anisotropic with brownish to greenish rotation tints. Internal reflections are absent. Reflectance values for the four COM wavelengths (R_{min}, R_{max} (%) (λ in nm)) are: 33.2, 37.8 (471.1); 31.8, 35.3 (548.3), 31.0, 34.7 (586.6); and 27.9, 32.5 (652.3). Electron microprobe analysis gave (in wt %, average of 5 spot analyses): Cu 2.33 (8), Ag 0.53 (5), Hg 0.98 (6), Tl 0.78 (3), Pb 44.06 (14), As 4.66 (7), Sb 23.90 (10), Bi 1.75 (7), total 99.38 (26). On the basis of 56 S atoms per formula unit, the chemical formula of ciriottiite is $Cu_{3.23(11)}Ag_{0.43(4)}Hg_{0.43(2)}Pb_{18.74(9)}Tl_{0.34(1)}Sb_{17.30(5)}As_{5.48(10)}Bi_{0.74(3)}S_{56}$. The main diffraction lines, corresponding to multiple *hkl* indices, are (*d* in Å (relative visual intensity)): 4.09 (m), 3.91 (m), 3.63 (vs), 3.57 (m), 3.22 (m), 2.80 (mw), 2.07 (s). The crystal structure study revealed ciriottiite to be monoclinic, space group $P2_1/n$, with unit-cell parameters a = 8.178 (2), b = 28.223 (6), c = 42.452 (5) Å, β = 93.55 (2)°, V = 9779.5 (5) Å^3, Z = 4. The crystal structure was refined to a final R_1 = 0.118 for 21304 observed reflections. Ciriottiite is the Cu analogue of sterryite and can be described as an expanded derivative of owyheeite. The name ciriottiite honors Marco Ernesto Ciriotti (b. 1945) for his longstanding contribution to mineral systematics.

Keywords: ciriottiite; owyheeite derivative; lead; copper; antimony; arsenic; Tavagnasco; Piedmont; Italy

1. Introduction

During the study of the mineral assemblage of the Pb-Bi-Zn-As-Fe-Cu ore district from Tavagnasco, Turin, Piedmont, Italy, several lead sulfosalts have been identified as accessory minerals. One specimen collected at the *Espérance superiore* tunnel (latitude 45.5416 N; longitude 7.8134 E) showed tubular crystals, up to 150 μm in length, in the vugs of quartz-carbonate veins. X-ray single-crystal diffraction study indicated a sterryite-like unit-cell, with a smaller unit-cell volume. Chemical analysis and the crystal structure refinement allowed the identification of this phase as the Cu-analogue of sterryite, ideally $Cu(Cu,Ag)_3Pb_{19}(Sb,As,Bi)_2(As_2)S_{56}$. This new mineral was named ciriottiite, in honor of Marco Ernesto Ciriotti (b. 1945), Italian member of the IMA CNMNC since 2013, president of the AMI (*Associazione Micromineralogica Italiana*, Italian Micromineralogical Association) since 2003, for his

contribution to mineral systematics. In addition, he is Associate Editor of MICRO (the AMI magazine) and coauthors of several papers on systematic and topographic mineralogy, and the book "Italian Type Minerals" [1]. The mineral and its name have been approved by the IMA CNMNC, under the number 2015-027 [2]. The holotype specimen of ciriottiite is deposited in the mineralogical collections of the Museo di Storia Naturale, Università degli Studi di Firenze, Via G. La Pira 4, Florence, Italy, under catalogue number 3161/I.

The mineralogical description of ciriottiite, as well as its crystal structure, are described in this paper.

2. Geological Setting and Occurrence of Ciriottiite

The geological setting of the Tavagnasco Pb-Bi-Zn-As-Fe-Cu hydrothermal ore district, located about 50 km N of Turin, has been discussed in [3]. Ciriottiite occurs in a complex sulfide assemblage. The ore minerals are represented by chalcopyrite, arsenopyrite, galena, with minor amounts of bismuthinite, sulfosalts (cosalite, izoklakeite-giessenite, and a kobellite-like mineral), bismuth, and gold. A series of alteration minerals (anglesite, azurite, langite, and tavagnascoite) have been identified. Ciriottiite is exceptionally rare. Up to now, only one specimen has been identified. In the holotype specimen, ciriottiite is associated with arsenopyrite and a kobellite-like mineral, within a vug of a quartz vein.

3. Mineral Description and Physical Properties

Ciriottiite (Figure 1) occurs as black tubular crystals, up to 150 μm in length and few μm thick. Streak is black and the luster is metallic.

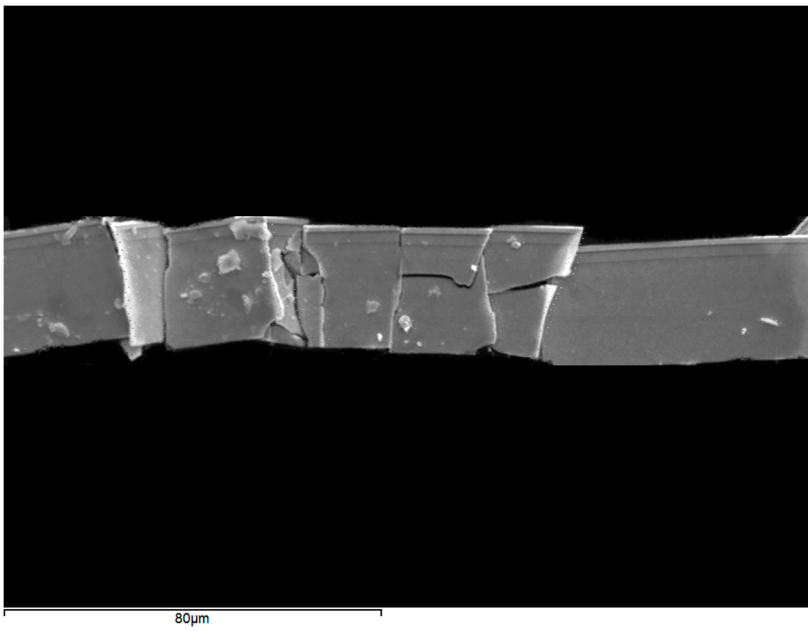

Figure 1. Backscattered electron image of ciriottiite obtained with a Scanning Electron Microscopy.

In plane-polarized incident light, ciriottiite is light grey in color. Under crossed polars, it is distinctly anisotropic, with brownish to greenish rotation tints. Internal reflections are absent and there is no optical evidence of growth zonation. Reflectance was measured in air using a Zeiss MPM-200 microphotometer (CRAIC Technologies, San Dimas, CA, USA) equipped with a MSP-20 system processor on a Zeiss Axioplan ore microscope. The filament temperature was approximately 3350 K. Readings were taken for specimen and standard (SiC) maintained under the same focus conditions. The diameter of the circular measuring area was 0.1 mm. Reflectance percentages in the form (R_{min},

R_{max} (%) (λ in nm)) are: 33.2, 37.8 (471.1); 31.8, 35.3 (548.3), 31.0, 34.7 (586.6); and 27.9, 32.5 (652.3). Such values are compared in Figure 2 to those measured on sterryite [4] and parasterryite [5].

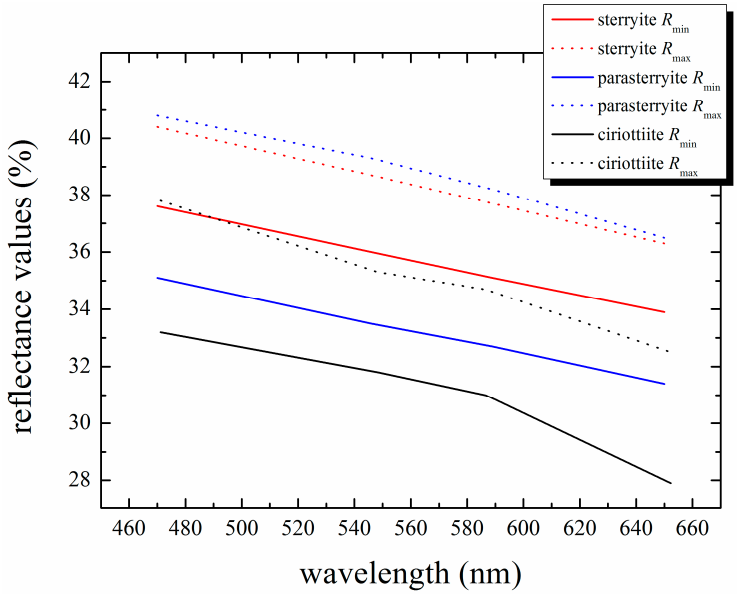

Figure 2. Reflectance values for ciriottiite (this study), sterryite [4] and parasterryite [5].

Ciriottiite is brittle. Its Vickers hardness (VHN_{10}) is 203 kg/mm^2 (range 190–219), corresponding to a Mohs hardness of ~3–3.5. On the basis of the empirical formula, the calculated density is 5.948 g/cm^3. The density on the basis of the ideal chemical formula is 5.918 g/cm^3.

3.1. Chemical Data

A preliminary EDS (Energy Dispersive Spectrometry) analysis performed on the crystal grain used for the structural study did not indicate the presence of elements (Z > 9) other than Cu, Pb, Bi, Sb, As, and S.

Quantitative chemical analysis were carried out using a JEOL JXA-8200 electron-microprobe (JEOL Instruments, Tokyo, Japan), operating in WDS (Wavelength Dispersive Spectrometry) mode. The experimental conditions were: accelerating voltage 20 kV, beam current 20 nA, beam size 1 μm. Counting times are 15 s for peak and 20 s for background. Standards are (element, emission line): Cu metal (Cu *Kα*), galena (Pb *Mα*), Bi metal (Bi *Mα*), synthetic TlBr (Tl *Mα*), synthetic Sb_2S_3 (Sb *Lα*), synthetic As_2S_3 (As *Lα*), pyrite (S *Kα*), Ag metal (Ag *Lα*), and cinnabar (Hg *Mα*). The crystal fragment was found to be homogeneous within analytical errors. Table 1 gives analytical data (average of 5 spot analyses).

Table 1. Chemical data of ciriottiite.

Element	wt (%) (*n* = 5)	Range	Estimated Standard Deviation
Cu	2.33	2.22–2.41	0.08
Ag	0.53	0.48–0.60	0.05
Hg	0.98	0.92–1.06	0.06
Tl	0.78	0.74–0.81	0.03
Pb	44.06	43.89–44.21	0.14
As	4.66	4.58–4.75	0.07
Sb	23.90	23.77–24.05	0.10
Bi	1.75	1.65–1.83	0.07
S	20.37	20.22–20.46	0.10
Total	99.38	98.94–99.61	0.26

The empirical formula, based on 56 S atoms per formula unit, is $Cu_{3.23(11)}Ag_{0.43(4)}Hg_{0.43(2)}Pb_{18.74(9)}Tl_{0.34(1)}Sb_{17.30(5)}As_{5.48(10)}Bi_{0.74(3)}S_{56}$. The analytical total is good; the calculated relative error on the valence equilibrium *Ev* (defined as *Ev* (%) = (*Ev* (+) − *Ev* (−)) × 100/*Ev* (−)) indicates a small excess of positive charges (average *Ev* (%) = 0.8 (3)).

3.2. Crystallography

For the X-ray single-crystal diffraction study, the intensity data were collected using an Oxford Diffraction Xcalibur 3 diffractometer, equipped with a Sapphire 2 CCD area detector, with Mo *Kα* radiation. The detector to crystal working distance was 6 cm. Intensity integration and standard Lorentz-polarization corrections were performed with the *CrysAlis* RED [6] software package. The program ABSPACK in *CrysAlis* RED [6] was used for the absorption correction. Tests on the distribution of $|E|$ values agree with the occurrence of an inversion centre ($|E^2 - 1| = 0.927$). This information, together with the systematic absences, suggested the space group $P2_1/n$. We decided to keep this non-standard setting of the space group to make easier the comparison with sterryite (see below). The refined unit-cell parameters are *a* = 8.178 (2), *b* = 28.223 (6), *c* = 42.452 (5) Å, β = 93.55 (2)°, *V* = 9779.5 (5) Å^3.

The crystal structure was refined with *Shelxl*-97 [7] starting from the atomic coordinates of sterryite [8], which represents the Ag-analogue of ciriottiite. The site occupancy factors (s.o.f.) were refined using the scattering curves for neutral atoms given in the *International Tables for Crystallography* [9]. Crystal data and details of the intensity data collection and refinement are reported in Table 2.

Table 2. Crystal and experimental details for ciriottiite.

Crystal Data	
Crystal size (mm^3)	0.040 × 0.045 × 0.060
Cell setting, space group	Monoclinic, $P2_1/n$
a, *b*, *c* (Å)	8.178 (2), 28.223 (6), 42.452 (5)
β (°)	93.55 (2)
V (Å^3)	9779.5 (5)
Z	4
Data Collection and Refinement	
Radiation, wavelength (Å)	Mo *Kα*, λ = 0.71073
Temperature (K)	293
$2\theta_{max}$ (°)	56.13
Measured reflections	172985
Unique reflections	22638
Reflections with $F_o > 4\sigma(F_o)$	21304
R_{int}	0.0578
$R\sigma$	0.0704
Range of *h*, *k*, *l*	$-10 \leqslant h \leqslant 10$, $-37 \leqslant k \leqslant 37$, $-55 \leqslant l \leqslant 55$
R ($F_o > 4\sigma(F_o)$)	0.1176
R (all data)	0.1194
wR (on F^2)	0.3187
GooF	1.159
Number of least-square parameters	960
Maximun and minimum residuals (*e*/Å^3)	9.60 (at 0.87 from As28), −8.26 (at 1.00 from As28)

After several cycles of isotropic refinement, the R_1 converged to 0.19, thus confirming the correctness of the structural model. Forty-seven cation and fifty-six anion sites occur in the crystal structure of ciriottiite. Mixed (Pb/Sb) and (Sb/As) sites have been detected, as well as mixed (Cu,Ag,Hg), (Cu,Hg), and (Cu/Bi) sites. The s.o.f. of the Ag34 site was identical to that observed in sterryite, being a mixed (Cu,Ag,Hg) site. Cu is the dominant cation at the former Ag25 of sterryite (now the site is labelled Cu25), probably partially substituted by Hg; Cu is also present at the former

split Ag33 site of sterryite (now the site is labelled Cu33), partially replaced by Bi. Bismuth was, moreover, attributed to the Pb7 site, the smallest Pb site in the ciriottiite structure. Thallium was not located, but it is likely hosted at one of the largest Pb sites (*i.e.*, Pb1–Pb6 sites). Refining the crystal structure assuming an anisotropic model for cations (but for the Cu33a/Bi33b split pair that resulted negatively defined), the R_1 dropped to 0.12. Finally, the refinement converged to 0.118 for 21304 observed reflections with ($F_o > 4\sigma$ (F_o)) assuming the anisotropic displacement parameters for all the atom positions (with the exception of the split pair Cu33a/Bi33b). Notwithstanding a good refinement of all the atom positions, including the lighter ones (S atoms), and reasonable bond distances, the residual factor *R* remained rather high, with relatively high residuals in the difference-Fourier map. A similar situation was observed in sterryite [8], as well as in other complex lead sulfosalts (see Table 2 in [8]), and probably reflects substitution issues.

The crystal structure refinement pointed to the crystal chemical formula $Cu_{0.80}(Cu_{1.93}Hg_{0.47}Ag_{0.40}Bi_{0.20})_{\Sigma 3.00}Pb_{15}(Pb_{3.89}Sb_{1.71}Bi_{0.40})_{\Sigma 6}Sb_{10}(Sb_{5.63}As_{4.37})_{\Sigma 10}(As_2)S_{56}$. This formula is not perfectly charge-balanced, showing an excess of charges (*Ev* (%) = +0.70), probably related to the non-localization of minor Tl^+, assumed as Pb^{2+} owing to the very similar scattering factor. With respect to the chemical data, the formula derived through the crystal structure refinement shows a lower Cu content (2.73 *apfu*, to be compared with 3.23 *apfu* from electron-microprobe analysis) and a lower Sb/As atomic ratio (2.72 to be compared with 3.15). Finally, a lower amount of Bi has been localized, even if some additional Bi could be hosted at Pb8 (~0.2 Bi *apfu*).

In order to propose an ideal chemical formula for ciriottiite, the occurrence of 0.34 *apfu* Tl replacing Pb cannot be neglected. Consequently, the chemical formula derived from the crystal structure refinement could be conveniently written as $Cu_{0.80}(Cu_{1.93}Hg_{0.47}Ag_{0.40}Bi_{0.20})_{\Sigma 3.00}(Pb_{14.65}Tl_{0.35})_{\Sigma 15}(Pb_{3.89}Sb_{1.71}Bi_{0.40})_{\Sigma 6}Sb_{10}(Sb_{5.63}As_{4.37})_{\Sigma 10}(As_2)S_{56}$. Taking into account the heterovalent substitutions $Cu^+ + Pb^{2+} = \gamma + Sb^{3+}$, $Cu^+ + Sb^{3+} = Hg^{2+} + Pb^{2+}$, $Cu^+ + 2Sb^{3+} = Bi^{3+} + 2Pb^{2+}$, $Tl^+ + Sb^{3+} = 2Pb^{2+}$, and the homovalent substitutions $Ag^+ = Cu^+$ and $Bi^{3+} = Sb^{3+}$, one obtains the formula $CuCu_3Pb_{18.57}(Sb,As)_{22.43}As_2S_{56}$, ideally $CuCu_3Pb_{19}(Sb,As)_{22}(As_2)S_{56}$.

The X-ray powder diffraction pattern, based on this structural model and calculated using the software *PowderCell* 2.3 [10], is given in Table 3. Owing to the uniqueness of the available crystal used for the single-crystal X-ray diffraction study and to the fact it was subsequently embedded in epoxy and polished for electron-microprobe analysis, X-ray powder pattern was not collected.

Table 3. Calculated X-ray powder diffraction data for ciriottiite. Only reflections with $I_{calc} > 10$ are listed. The five strongest reflections are given in bold.

I_{calc}	d_{calc}	*h k l*	I_{calc}	d_{calc}	*h k l*
11	10.59	0 0 4	20	2.939	2 5 6
13	4.237	0 0 10	54	2.936	0 8 8
25	4.113	0 6 5	37	2.928	2 2 9
20	4.058	0 2 10	14	2.877	−2 1 11
15	3.920	2 2 0	20	2.871	−2 5 8
14	3.916	0 4 9	22	2.868	2 7 0
11	3.897	−2 2 2	21	2.859	−2 7 2
12	3.816	0 1 11	27	2.854	2 6 5
15	3.714	0 6 7	22	2.852	2 3 9
26	3.652	2 3 2	33	2.833	−2 2 11
100	3.641	0 7 5	12	2.823	0 8 9
35	3.595	−2 3 4	36	2.800	−2 6 7
18	3.562	2 1 5	28	2.796	2 2 10
20	3.531	0 0 12	16	2.764	−2 3 11
12	3.517	0 6 8	12	2.739	2 7 4
17	3.459	−2 1 7	19	2.705	−2 2 12
14	3.442	2 0 6	20	2.698	0 9 8

Table 3. *Cont.*

I_{calc}	d_{calc}	*h k l*	I_{calc}	d_{calc}	*h k l*
15	3.407	−2 4 4	19	2.670	−2 8 1
13	3.334	−2 0 8	23	2.313	2 10 1
12	3.299	2 4 4	22	2.303	−2 10 3
19	3.257	0 8 5	11	2.213	0 7 16
82	3.238	0 1 13	18	2.120	0 7 17
57	3.208	0 7 8	78	2.043	−4 0 2
11	3.205	2 2 7	16	2.036	0 8 17
13	3.176	0 2 13	15	1.996	0 14 3
27	3.030	2 5 5	12	1.895	2 6 17
10	3.009	0 1 14	11	1.771	−4 7 7
14	2.977	2 1 9	11	1.702	−4 1 15
24	2.966	−2 5 7	12	1.692	0 1 25

4. Crystal Structure Description

4.1. General Features

Owing to the large number of independent atom positions in the unit-cell, atom coordinates and displacement parameters for ciriottiite are given in the CIF, available as Supplementary material.

The crystal structure of ciriottiite is topologically identical with that of sterryite [8]. It is composed by the fishbone arrangement of complex columns along **b**. These complex columns have been delimited by dotted lines in Figure 3 and they have been defined taking into account the surfaces of weakest bonding, cutting the longest (Sb/As)–S bonds along distinct lone-electron-pair micelles.

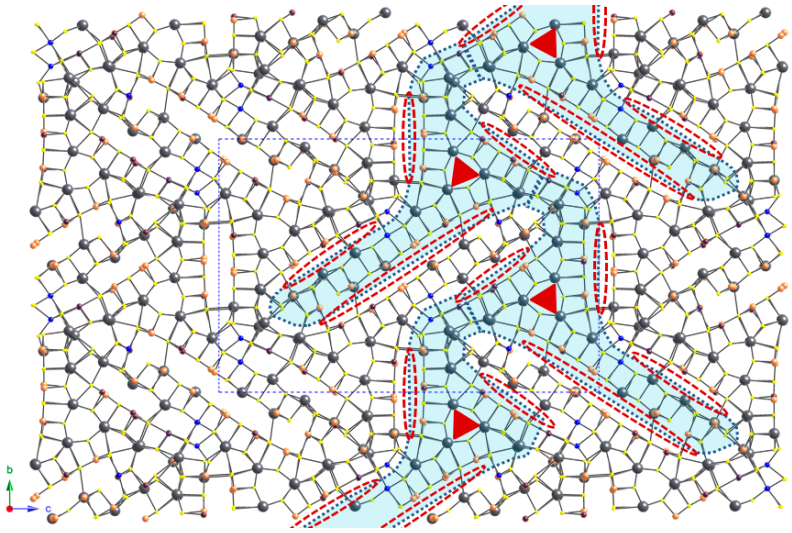

Figure 3. Projection of the crystal structure of ciriottiite, as seen down **a**. The fishbone layer along **b**, formed by the connection of complex columns, is shaded in light blue. Red ellipses (dotted lines) symbolize the lone-electron-pair micelles of (Sb/As) atoms. Red triangles show the pseudotrigonal organization of the prismatic core of the complex columns. Circles: grey = Pb sites; orange = Sb sites; violet = As sites; blue = Cu sites; yellow = S sites.

A single kind of complex column, corresponding to one unit formula, occurs in ciriottiite. It has a pseudotrigonal prismatic core and two "arms" (=ribbon projections) of unequal length (Figure 4), *i.e.*, short and long arms. Each complex column contains 16 Pb sites (with minor Bi and Tl), 10 pure Sb sites, 10 mixed (Sb/As) sites (five having As > Sb), and five mixed (Pb/Sb) positions (one having Sb > Pb).

As in sterryite, one of the mixed (Pb,Sb) position (*i.e.*, Pb44) located on the short arm is connected to a partially occupied Cu site (*i.e.*, Cu43) in such a way that the Cu s.o.f. (0.80) is very close to the Pb s.o.f. (0.81), corresponding to the substitution rule $^{Pb44}Pb^{2+} + {}^{Cu43}Cu^{+} = {}^{Pb44}Sb^{3+} + {}^{Cu43}\gamma$. In the short arm there are two pure As sites, forming localized As–As bonds characterizing both ciriottiite and sterryite (Figure 4a).

The other Cu-hosting sites are located in the long arm. At its base, a mixed and split (Cu/Bi) site, namely Cu33, alternates with a mixed (Cu,Ag,Hg) site (Cu34); the former corresponds to a split (Cu/Ag) site in sterryite [8] (Figure 4b). At the end of the long arm, a (Cu,Hg) site (Cu25) alternates with a mixed (Sb,As) site (Sb26) (Figure 4c); in sterryite, as well as in parasterryite and meerschautite [8,11], a similar configuration with an (Ag,Cu) site alternating with an Sb one was reported [8].

As in the crystal structure descriptions of sterryite and parasterryite [8], each column has been delimited by three faces denoted *A*, *B*, and *C* (more details in [8]); these different faces control the polymerization of (Sb/As) sites with S.

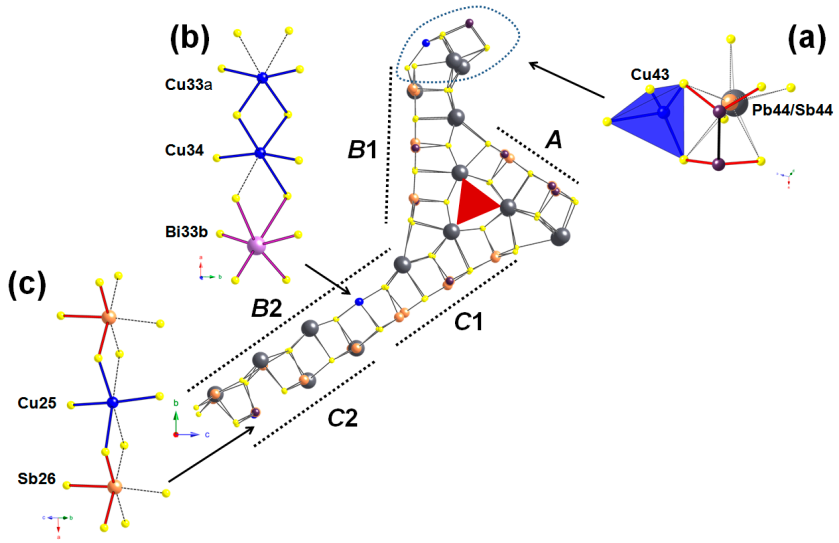

Figure 4. The fundamental building block of ciriottiite as seen down **a**. The pseudo-trigonal rod is highlighted. The *A*, *B*1, *B*2, *C*1, and *C*2 faces are shown. Some structural features discussed in the text are shown in (**a**)–(**c**). Same symbols as in Figure 3. In addition, light violet circle = Bi site.

4.2. Cation Coordination and Site Occupancies

Owing to the large number of Pb, Sb, and As sites occurring in the crystal structure of ciriottiite, their coordination will be not detailed here. Pb sites display a coordination number ranging from 6 to 9, as in sterryite [8]. The bond-valence sums (BVS) for pure Pb sites, calculated using the bond parameters given in [12] and expressed in valence unit (v.u.), range between 1.89 (Pb30) and 2.43 v.u. (Pb7). The oversaturation of the latter was interpreted as due to minor Bi replacing Pb and the s.o.f. ($Pb_{0.60}Bi_{0.40}$) was assumed; minor amounts of Bi could additionally be hosted at the Pb8 site, having a BVS of 2.25 v.u. Sb and As sites usually show a triangular pyramidal coordination (taking into account only the shortest *Me*–S distances); their BVSs range between 2.75 (Sb29) and 3.60 v.u. (Sb42). In ciriottiite, these sites usually result overbonded; following the bond-valence method used during the crystal structure study of sterryite and parasterryite [8], this oversaturation could indicate the occurrence of an As content larger than those found both during electron-microprobe analysis and crystal structure refinement, *i.e.*, *ca.* 6.9 As *apfu*. Mixed (Pb/Sb) sites display usually a six-fold coordination; if split, the Sb position usually has only two distances shorter than 2.70 Å, as a result of its average position.

In the short arm, the Cu43 site has a distorted tetrahedral coordination, with three short distances ranging between 2.25 and 2.30 Å, and a longer one at 2.57 Å. Its BVS, calculated assuming the

refined s.o.f., is 0.89 v.u. In the same arm, the As46 and As47 sites are at short distance along **a**, *i.e.*, 2.63 Å, forming an As–As pair. Each As atom of this pair is bonded to two S atoms, thus forming an $(As_2)S_4$ group, analogous to that occurring in sterryite [8] and similar to those reported in several As sulfides (e.g., alacranite [13], bonazziite [14], realgar [15], uzonite [16], wakabayashilite [17]) and in dervillite [18].

The two Cu sites located at the base of the long arm, *i.e.*, Cu33 and Cu34, have mixed occupancies. Cu33 is actually split into two sub-positions, Cu33a and Bi33b. Cu33a has a coordination close to a linear one, with two S atoms at 2.43 and 2.44 Å. Other two S atoms are located at 2.77 and 2.89 Å; the Cu33a coordination is completed by two additional S at 3.08 and 3.10 Å. The Bi33b position has been tentatively assigned to Bi. The coordination environment can be described as a distorted octahedron, with distances ranging from 2.47 to 3.46 Å. Actually, a Bi–S distance of 2.47 Å is too short and results in an oversaturation of the Bi atom at the Bi33b position (4.22 v.u. instead of the theoretical 3.00 v.u.). In our opinion, the positions of the S atoms bonded to the split pair Cu33a/Bi33b are only average positions. Indeed, assuming a full-occupancy of Cu at the Cu33a site, a BVS of 0.64 v.u. is obtained, thus indicating a too large site for a pure Cu site. Assuming a mixed (Cu,Bi) population, the weighted BVS is 1.35 v.u., to be compared with a theoretical value of 1.40 v.u. calculated on the basis of the refined s.o.f. ($Cu_{0.80}Bi_{0.20}$). Cu34 corresponds to a mixed (Cu,Ag,Hg) site, as in sterryite [8]. It displays two short distances (*Me*–S distances of 2.48 and 2.58 Å), arranged in a linear coordination, and four additional longer ones (three ranging between 2.81 and 2.96 Å, and a fourth one at 3.22 Å). This polyhedron is similar to that reported in sterryite [8]; the average <Cu34–S> distance is 2.81 Å. The BVS at the Cu34 site is 1.10 v.u.; the theoretical value, calculated on the basis of the assumed s.o.f. ($Cu_{0.40}Ag_{0.40}Hg_{0.20}$) should be 1.20 v.u.

At the end of the long arm, Cu25 site displays a strongly distorted octahedral coordination, close to a linear one. Indeed, two S atoms are at 2.39 and 2.43 Å from the metal position; other two are located at 2.64 and 2.74. The remaining S atoms are at very long distances, *i.e.*, 3.53 and 3.58 Å. The site occupancy at Cu25 has been interpreted as a mixed (Cu,Hg). The BVS is 1.15 v.u., to be compared with the theoretical value 1.27 v.u. calculated on the basis of the refined s.o.f. ($Cu_{0.73}Hg_{0.27}$).

4.3. Polymerization of (Sb/As) Sites

The examination of the organization of the (Sb/As) sites into finite $Me^{3+}{}_mS_n$ chain fragments (hereafter "polymers") is possible by taking into account only the shortest Me^{3+}–S bond distances (*Me*–S distances shorter than 2.70 Å [8]).

On the face *A* (Figure 5a), a central squared Me_2S_4 group (where $Me = Sb_{1.92}As_{0.08}$), is edged by two MeS_3 groups, with $Me = (Sb_{0.66}As_{0.34})$ and $(As_{0.58}Sb_{0.42})$, respectively.

On sub-surface *B*1 (Figure 5b), there are two peripheral MeS_3 groups, with *Me* having composition $(As_{0.72}Sb_{0.28})$ and Sb, respectively. The central portions are formed by two distinct polymers. One of the sites involved in these polymers is actually a mixed (Sb,Pb) site. If Pb is absent, there are two open Me_2S_4 groups, with $Me = (Sb_{1.36}As_{0.64})$ and $Sb_{2.00}$, respectively. On the contrary, if Pb occurs, the central portion of the *B*1 sub-surface shows an Me_2S_4 polymer and an isolated SbS_3 group.

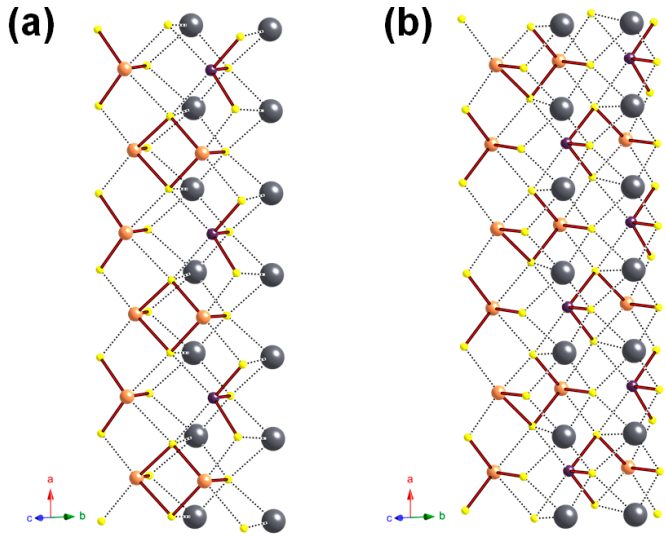

Figure 5. (Sb/As)–S polymerization along the *A* (**a**); and *B*1 (**b**) surfaces. Shortest (Sb/As)–S bonds are shown as thick red lines; dotted lines represent longer (Sb/As)–S bonds and other *Me*–S bonds. Circles: same symbols as in Figures 3 and 4.

Along the *C*1 sub-surface (Figure 6a), an asymmetric sequence of MeS_3, open Me_2S_4, and a crankshaft chain Me_3S_7. Me occupancies correspond to Sb, $(Sb_{1.93}As_{0.07})$, and $(Sb_{1.66}As_{1.34})$, respectively.

The $(Sb/As)_mS_n$ polymers in the outer part of the long arm concerns the two atom sub-surfaces *B*2 and *C*2 (Figure 6b). In ciriottiite, there are three mixed (Pb,Sb) positions (Pb22, Pb23, and Pb27). Neglecting the minor Sb content of these sites, three Me_mS_n groups can be highlighted, *i.e.*, MeS_3, a stretched Me_2S_4, and a Me_2S_5 group, with *Me* corresponding to Sb, $Sb_{2.00}$, and $(Sb_{1.40}As_{0.60})$, respectively.

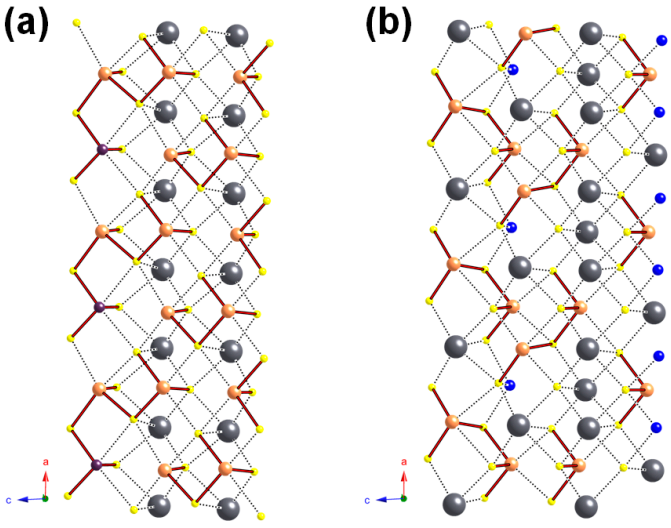

Figure 6. (Sb/As)–S polymerization along the *C*1 (**a**); and *B*2/*C*2 (**b**) surfaces. Same symbols as in Figures 3–5.

Such a polymeric organization closely corresponds to that reported for sterryite [8].

5. Discussion

5.1. Ciriottiite in the Framework of the Owyheeite Group and Its Comparison with Sterryite

Ciriottiite is the Cu-analogue of sterryite, $Cu(Ag,Cu)_3Pb_{19}(Sb,As)_{22}(As_2)S_{56}$. It is an expanded derivative of owyheeite, belonging to the owyheeite group (Table 4).

Table 4. Members of the owyheeite group.

Mineral	*a* (Å)	*b* (Å)	*c* (Å)	β (°)	*V* (Å^3)	Space Group	Ref.
Ciriottiite	8.178	28.223	42.452	93.55	9780	$P2_1/n$	*This work*
Meerschautite	8.2393	43.6015	28.3688	94.128	10165	$P2_1$	[11]
Owyheeite	4.1035	27.3144	22.3966	90.359	2571	$P2_1/c$	[19]
Parasterryite	8.3965	27.954	43.884	90.061	10300	$P2_1/c$	[8]
Sterryite Madoc	28.4	42.6	8.26	90	9921	*Pba*2 or *Pbam*	[20]
Sterryite Pollone	8.1891	28.5294	42.98	94.896	10005	$P2_1/n$	[8]
Tubulite	4.132 (×2)	43.1	27.4	93.2	4872 (×2)	$P2/c$, *Pc* or $P2_1/c$	[21]

All these sulfosalts are characterized by crystal structures built around a pseudotrigonal core, relating them to the zinkenite plesiotypic series (sulfosalts of the cyclic rod-type and derivatives [22,23]).

The substitution of Cu for Ag was reported in sterryite from the Pollone mine. Indeed, two chemical varieties were described, *i.e.*, Sb-rich and Sb-poor sterryite. Actually, the Sb-rich sterryite is also Cu-rich, with a Cu/(Cu + Ag + Hg) atomic ratio of 0.464. to be compared with 0.230 in Sb-poor sterryite. Ciriottiite is definitely enriched in Cu, with a Cu/(Cu + Ag + Hg) atomic ratio of 0.788. The As/(As + Sb + Bi) atomic ratio is 0.240, close to the value reported for Sb-rich sterryite, *i.e.*, 0.259; Sb-poor sterryite is As-enriched, with an As/(As + Sb + Bi) atomic ratio of 0.392. Consequently, ciriottiite appears as being a Cu-dominant Sb-rich sterryite. This chemical difference is reflected in the smaller unit-cell volume of the former, showing a volume contraction of *ca.* −2.25%, probably as result of the substitution of Ag with Cu, having a smaller atomic radius (1.00 *vs.* 0.60 Å, respectively).

5.2. The Study of Sulfosalts as a Proxy for Unraveiling Ore Geochemistry

Sulfosalts are a heterogeneous group of compounds relatively common as accessory minerals in hydrothermal veins. Many species have very complex chemistry and in some cases minor chemical components appear fundamental for their stabilization. Only an accurate knowledge of their crystal structures allows the understanding of the role of such minor components in these compounds, giving interesting insights into the ore geochemistry. Indeed, the crystal chemistry of the sulfosalts occurring in a hydrothermal vein is mainly controlled by the chemistry of the hydrothermal fluids. Therefore, the characterization of sulfosalt assemblage could give interesting information about the ore geochemistry. In other cases, some structural features could indicate particular crystallization conditions, like the presence of chlorine site (e.g., dadsonite [24]), indicating the high chlorinity of the hydrothermal solutions, or localized S–S bonds, indicating high $f(S_2)$ conditions (e.g., moëloite [25]).

The occurrence of the As–As pair in ciriottiite, revealed through the crystal structure solution, indicates a S deficit, *i.e.*, a low $f(S_2)$ in the crystallization medium; probably, such a relatively low $f(S_2)$ allows the stabilization of ciriottiite, explaining its extreme rarity in nature, as hypothesized for sterryite [4]. In addition, the Cu-rich nature of this new mineral with respect to sterryite is related to the Cu-rich nature of the Tavagnasco ore district, with the occurrence of chalcopyrite as one of most important sulfides forming the ore deposits. Ciriottiite is thus a multicomponent compound belonging ideally to the pseudo-quinary system PbS–Sb_2S_3–As_2S_3–Cu_2S–AsS.

Supplementary Materials: The following is available online at www.mdpi.com/2075-163X/6/1/8/s1, CIF: ciriottiite.

Acknowledgments: The research was supported by "progetto d'Ateneo 2013, University of Firenze" to Luca Bindi.

Author Contributions: Luca Bindi and Cristian Biagioni conceived and designed the experiments; Luca Bindi performed the experiments; Luca Bindi and Cristian Biagioni analyzed the data; Bruno Martini and Adrio Salvetti found the new mineral; Luca Bindi and Cristian Biagioni wrote the paper.

Conflicts of Interest: The authors declare no conflict of interest.

References

1. Ciriotti, M.E.; Fascio, L.; Pasero, M. *Italian Type Minerals*; Edizioni Plus: Pisa, Italy, 2009; p. 360.
2. Bindi, L.; Biagioni, C.; Martini, B.; Salvetti, A. Ciriottiite, IMA 2015-027. CNMNC Newsletter No. 26, August 2015, page 943. *Miner. Mag.* **2015**, *79*, 941–947.
3. Bindi, L.; Biagioni, C.; Martini, B.; Salvetti, A.; Dalla Fontana, G.; Taronna, M.; Ciriotti, M.E. Tavagnascoite, $Bi_4O_4(SO_4)(OH)_2$, a new oxy-hydroxy bismuth sulfate related to klebelsbergite. *Miner. Mag.* **2016**. [CrossRef]
4. Jambor, J.L. New lead sulfantimonides from Madoc, Ontario. 1. *Can. Miner.* **1967**, *9*, 7–24.
5. Moëlo, Y.; Orlandi, P.; Guillot-Deudon, C.; Biagioni, C.; Paar, W.; Evain, M. Lead-Anitmony sulfosalts from Tuscany (Italy). XI. The new mineral species parasterryite, $Ag_4Pb_{20}(Sb_{14.5}As_{9.5})S_{24}S_{58}$, and associated sterryite, $Cu(Ag,Cu)_3Pb_{19}(Sb,As)_{22}(As–As)S_{56}$, from the Pollone mine, Tuscany, Italy. *Can. Miner.* **2011**, *49*, 623–638. [CrossRef]
6. Oxford Diffracxtion. *CrysAlis RED (Version 1.171.31.2) and ABSPACK in CrysAlis RED*; Oxford Diffraction Ltd.: Oxfordshire, England, UK, 2006.
7. Sheldrick, G.M. A short history of SHELX. *Acta Crystallogr.* **2008**, *A64*, 112–122. [CrossRef]
8. Moëlo, Y.; Guillot-Deudon, C.; Evain, M.; Orlandi, P.; Biagioni, C. Comparative modular analysis of two complex sulfosalt structures: Sterryite, $Cu(Ag,Cu)_3Pb_{19}(Sb,As)_{22}(As–As)S_{56}$, and parasterryite, $Ag_4Pb_{20}(Sb,As)_{24}S_{58}$. *Acta Crystallogr.* **2012**, *B68*, 480–492. [CrossRef] [PubMed]
9. Wilson, A.J.C., Ed.; *International Tables for Crystallography. Volume C: Mathematical, Physical and Chemical Tables*; Kluwer Academic: Dordrecht, The Netherland, 1992.
10. Kraus, W.; Nolze, G. PowderCell—A program for the representation and manipulation of crystal structures and calculation of the resulting X-ray powder patterns. *J. Appl. Crystallogr.* **1996**, *29*, 301–303. [CrossRef]
11. Biagioni, C.; Moëlo, Y.; Orlandi, P.; Stanley, C. Lead-antimony sulfosalts from Tuscany (Italy). XVII. Meerschautite, $(Ag,Cu)_{5.5}Pb_{42.4}(Sb,As)_{45.1}S_{112}O_{0.8}$, a new expanded derivative of owyheeite from the Pollone mine, Valdicastello Carducci: Occurrence and crystal structure. *Miner. Mag.* **2016**. [CrossRef]
12. Brese, N.E.; O'Keeffe, M. Bond-valence parameters for solids. *Acta Crystallogr.* **1991**, *B47*, 192–197. [CrossRef]
13. Bonazzi, P.; Bindi, L.; Popova, V.; Pratesi, G.; Menchetti, S. Alacranite, As_8S_9: Structural study of the holotype and re-assignment of the original chemical formula. *Am. Miner.* **2003**, *88*, 1796–1800. [CrossRef]
14. Bindi, L.; Pratesi, G.; Muniz-Miranda, M.; Zoppi, M.; Chelazzi, L.; Lepore, G.O.; Menchetti, S. From ancient pigments to modern optoelectronic applications of arsenic sulfides: Bonazziite, the natural analogue of β-As_4S_4 from Khaidarkan deposit, Kyrgyzstan. *Miner. Mag.* **2015**, *79*, 121–131. [CrossRef]
15. Mullen, D.J.E.; Nowacki, W. Refinement of the crystal structure of realgar, AsS and orpiment, As_2S_3. *Z. Kristallogr.* **1972**, *136*, 48–65. [CrossRef]
16. Bindi, L.; Popova, V.; Bonazzi, P. Uzonite, As_4S_5, from the type locality: Single-crystal X-ray study and effects of exposure to light. *Can. Miner.* **2003**, *41*, 1463–1468. [CrossRef]
17. Bonazzi, P.; Lampronti, G.I.; Bindi, L.; Zanardi, S. Wakabayashilite, $[(As,Sb)_6S_9][As_4S_5]$: Crystal structure, pseudosymmetry, twinning, and revised chemical formula. *Am. Miner.* **2005**, *90*, 1108–1114. [CrossRef]
18. Bindi, L.; Nestola, F.; De Battisti, L.; Guastoni, A. Dervillite, Ag_2AsS_2, from Lengenbach quarry, Binn valley, Switzerland: Occurrence and crystal structure. *Miner. Mag.* **2013**, *77*, 3105–3112. [CrossRef]
19. Laufek, F.; Pažout, R.; Makovicky, E. Crystal structure of owyheeite, $Ag_{1.5}Pb_{4.43}Sb_{6.07}S_{14}$: Refinement from powder synchrotron X-ray diffraction. *Eur. J. Miner.* **2007**, *19*, 557–566. [CrossRef]
20. Jambor, J.L. New lead sulfantimonides from Madoc, Ontario. 2. Mineral descriptions. *Can. Miner.* **1967**, *9*, 191–213.
21. Moëlo, Y.; Pecorini, R.; Ciriotti, M.E.; Meisser, N.; Caldes, M.T.; Orlandi, P.; Petit, P.E.; Martini, B.; Salvetti, A. Tubulite—$Ag_2Pb_{22}Sb_{20}S_{53}$, a new Pb–Ag–Sb sulfosalt from Le Rivet quarry, Peyrebrune ore field (Tarn, France) and Biò, Borgofranco mines, Borgofranco d'Ivrea (Piedmont, Italy). *Eur. J. Miner.* **2013**, *25*, 1017–1030.
22. Makovicky, E. Cyclically twinned sulphosalt structures and their approximate analogues. *Z. Kristallogr.* **1985**, *173*, 1–23. [CrossRef]

23. Moëlo, Y.; Makovicky, E.; Mozgova, N.N.; Jambor, J.L.; Cook, N.; Pring, A.; Paar, W.H.; Nickel, E.H.; Graeser, S.; Karup-Møller, S.; *et al*. Sulfosalt systematics: A review. Report of the sulfosalt sub-committee of the IMA Commission on Ore Mineralogy. *Eur. J. Miner.* **2008**, *20*, 7–46. [CrossRef]
24. Makovicky, E.; Topa, D.; Mumme, W.G. The crystal structure of dadsonite. *Can. Miner.* **2006**, *44*, 1499–1512. [CrossRef]
25. Orlandi, P.; Meerschaut, A.; Palvadeau, P.; Merlino, S. Lead-antimony sulfosalts from Tuscany (Italy). V. Definition and crystal structure of moëloite, $Pb_6Sb_6S_{14}(S_3)$, a new mineral from the Ceragiola marble quarry. *Eur. J. Miner.* **2002**, *14*, 599–606. [CrossRef]